

# X-Ray Investigating the Aging Process of Aluminum Hydroxide Adjuvant in Protein-Based Vaccine Formulations Over a Short Period

Mohammad Reza Halvagar<sup>\*1</sup>, Mohammad Zali<sup>1 and 2</sup>, Sara Zali<sup>3</sup>, Mahdiah Najafi Mobarra<sup>2</sup>, Samira Bahemat<sup>1</sup>

1. Department of Inorganic Chemistry, Chemistry and Chemical Engineering Research Center of Iran, PO Box 14335-186, Tehran, Iran
2. Chemistry Department, Razi Vaccine & Serum Research Institute, Agricultural Research, Education and Extension Organization (AREEO), Karaj, Iran
3. Quality Assurance Department, Razi Vaccine & Serum Research Institute, Agricultural Research, Education and Extension Organization (AREEO), Karaj, Iran

Corresponding author. Tel.: +98 9123891981,  
E-mail address: halvagar@ccerci.ac.ir

## Abstract:

Nearly a century has passed since Glenny and colleagues introduced aluminum-based adjuvants. Over this extensive period, billions of doses of human and veterinary vaccines incorporating these adjuvants have been produced, ensuring both human health and food security. Aluminum-based adjuvants have played a pivotal role during epidemics, allowing scientists to accelerate vaccine development and save lives. Continuous research conducted by institutions worldwide has substantiated the safety and efficacy of aluminum-based adjuvants, establishing them as the gold standard. Consequently, any new adjuvant must be benchmarked against aluminum-based adjuvants and demonstrate substantial advantages to gain regulatory approval.

This study aims to investigate the short-term structural and physicochemical changes of aluminum hydroxide in protein-based formulations under thermal treatments at 100°C for 24, 48, and 72 hours. These periods were designed to simulate the aging process that occurs during the storage of adjuvants at room temperature. Specifically, the research examines changes in the physicochemical properties of the adjuvant, including pH fluctuations during these thermal treatments, alterations during the sterilization process, protein adsorption capacity for each sample, particle size distribution, and X-ray diffraction (XRD) patterns. These findings not only enhance our understanding of adjuvant stability in vaccine formulations but also provide valuable insights for determining their optimal shelf life and performance.

36 The study demonstrates that the best storage conditions for the adjuvant, with minimal impact from  
37 the aging process, are a low pH (pH=5) and higher ionic strength. It was also confirmed that  
38 innovative measures, such as reducing the sterilization cycle, stirring the samples after  
39 sterilization, and rapidly cooling them afterward, can prevent crystal growth and even produce  
40 smaller particle sizes with higher adjuvanticity. This is significant as previous studies had reported  
41 a decline in adjuvanticity following sterilization.

42  
43 Keywords: X-ray diffraction (XRD), aluminum hydroxide adjuvant stability, aging process  
44 simulation, protein adsorption capacity, particle size distribution, sterilization effects on adjuvants,  
45 vaccine adjuvant optimization, ionic strength and adjuvant stability Vaccine formulation.

46

47

48

## 49 **1. Introduction**

50 Vaccination is one of the most effective strategies for the prevention and control of infectious  
51 diseases, safeguarding the health of billions over several decades. Beyond individual protection,  
52 vaccines contribute significantly to reducing mortality rates, particularly among children, and ease  
53 the burden on healthcare systems worldwide. For instance, vaccines against diseases like measles  
54 and polio have led to remarkable declines in childhood mortality and have prevented countless  
55 hospitalizations, especially in low-resource regions (1).

56 Veterinary vaccines have also played a crucial role by controlling animal diseases, especially  
57 zoonotic diseases, thereby enhancing food security and reducing human exposure to these  
58 pathogens (2). This protection extends to broader economic impacts, as the prevention of disease  
59 outbreaks through vaccination reduces healthcare costs, improves population productivity, and  
60 stabilizes economies—an effect observed during the COVID-19 pandemic and other significant  
61 outbreaks (3).

62 Vaccines consist of two essential components: antigens and adjuvants. Antigens form the  
63 biological part of the vaccine, representing the pathogen, enabling the immune system to recognize  
64 and prepare to combat the actual pathogen. Adjuvants assist by presenting antigens more  
65 effectively to the immune system, thereby enhancing the immune response (4). In many vaccines,  
66 especially newer formulations, the immune system may not effectively recognize the antigen

without the presence of an adjuvant. Adjuvants make it possible for vaccines to achieve the necessary immunogenicity with smaller amounts of antigen. Additionally, they enhance immune responses through various mechanisms.

The concept of adjuvants in vaccine formulations dates back nearly a century, with the introduction of aluminum salts as the first adjuvants by Alexander Glenny (5) and his colleagues in 1926. They discovered that aluminum-based compounds could significantly enhance the immune response to diphtheria toxoid, allowing for stronger and longer-lasting immunity with lower doses of antigen. This early finding set the foundation for adjuvant research, highlighting the role of adjuvants in boosting vaccine efficacy and reducing the amount of antigen required for effective immunization. Over time, pathogens have become increasingly complex, and with the emergence of new strains, antigens need to be updated and often made more sophisticated. This means that today's expectations from adjuvants have far surpassed the initial expectations set by Glenny (5) and his colleagues in 1926. However, aluminum-based adjuvants continue to be widely used in numerous vaccines, having maintained their status as the dominant adjuvant over nearly a century, to the point where they are now regarded as the "gold standard."

Today, multiple vaccine platforms are available, including inactivated, recombinant, and subunit vaccines. Correspondingly, various types of adjuvants, such as oil-based adjuvants (including water-in-oil (W/O) and oil-in-water (O/W) emulsions), squalene-based adjuvants, saponin adjuvants, and nano-based adjuvants, have been developed. Nevertheless, aluminum-based adjuvants continue to be predominant, even in many modern vaccines.

Adjuvant research can be seen as a reservoir for the future and a critical foundation for emergency preparedness. Developing adjuvants enables scientists and vaccine manufacturers to be well-prepared when confronted with emerging outbreaks. This readiness was evident during the COVID-19 pandemic, where scientists focused on producing antigens and relied on pre-developed adjuvants to expedite vaccine availability. Notably, among the COVID-19 vaccines developed during the pandemic, those utilizing the inactivated platform predominantly incorporated aluminum-based adjuvants in their formulations.

In summary, the combination of safety, cost-effectiveness, stability, and proven efficacy in stimulating humoral immunity makes aluminum-based adjuvants ideal for many vaccine formulations. While research continues into developing adjuvants that also enhance cellular

immunity, aluminum adjuvants remain indispensable in modern vaccination programs, especially for routine and widely administered vaccines.

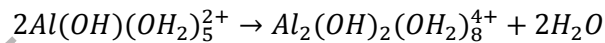
Despite nearly a century of use and research, there are still uncertainties regarding the exact mechanisms of action for aluminum-based adjuvants (6). Additionally, new adjuvants must demonstrate their efficacy and safety through comparison with aluminum-based adjuvants to receive regulatory approval. These factors make ongoing research into aluminum-based adjuvants essential (7).

One of the most well-known mechanisms is the "depot effect," in which aluminum-based adjuvants act as a reservoir, releasing the antigen gradually to elicit a prolonged immune response, reducing the need for additional booster doses. Consequently, adjuvants must be capable of physically or chemically binding to the antigen and delivering it to antigen-presenting cells following injection. This binding generally occurs on the antigen's surface, and adjuvant design often aims to establish electrostatic interactions between the adjuvant and antigen. As such, key characteristics like surface charge (or zeta potential) and surface area, which correspond to adjuvant size, are carefully controlled to optimize this binding.

Aluminum hydroxide adjuvants possess an amorphous structure that undergoes sequential deprotonation and dehydration reactions during the aging process (as shown in Eq. 1 and Eq. 2). These reactions lead to the formation of double hydroxide bridges, resulting in the release of  $H^+$  ions (8). Throughout this process, aluminum hydroxide transitions from an amorphous structure to a more crystalline form, such as poorly crystalline boehmite ( $AlOOH$ ).



Eq. 1. Deprotonation reaction during the aging process



Eq. 2. Dehydration reaction during the aging process

The development of double hydroxide bridges enhances the crystallinity and structural order of the material. Aluminum hydroxide, initially in an amorphous state, gradually transitions into a more crystalline form, such as  $AlOOH$  with low crystallinity. This structural ordering can be

127 clearly observed in the differences between the XRD patterns of the adjuvants before and after the  
128 aging process.

129 Fresh aluminum hydroxide adjuvants exhibit an amorphous structure, resulting in broad and low-  
130 intensity peaks in their XRD patterns. Gradually, as the structure of the adjuvant becomes more  
131 ordered and transitions into a semi-crystalline form, the peaks become sharper and more intense,  
132 while their width decreases.

133 The width-at-half-height (WHH) can be used as a reliable measure of aging. A lower WHH value  
134 indicates a more developed structure of the adjuvant, signifying that the sample has undergone a  
135 more extensive aging process (9).

136 The formation of each hydroxide bridge releases protons ( $H^+$ ) into the environment, leading to a  
137 gradual decrease in pH. This change plays a critical role in the aging process and impacts the  
138 material's stability.

139 As structural order increases and hydroxide bridges form, the available active surface area  
140 decreases. This reduction adversely affects the material's capacity to adsorb proteins or antigens,  
141 which is a key property influencing the performance of adjuvants in vaccine formulations (10).

142 Due to structural changes and increased crystalline order of aluminum hydroxide adjuvant during  
143 the aging process, the effective surface area of the adjuvant particles decreases, leading to a  
144 reduction in their protein adsorption capacity (11). For this evaluation, bovine serum albumin  
145 (BSA) with an isoelectric point of approximately 4.8 is used as the model protein, as the isoelectric  
146 point of aluminum hydroxide adjuvant is around 11. Consequently, under near-neutral pH  
147 conditions, the adjuvant and the model protein carry opposite charges, creating optimal conditions  
148 for assessing protein adsorption (12).

149 Thus, the aluminum hydroxide adjuvant subjected to the aging process can be evaluated by  
150 considering the following factors: Monitoring changes in the pH of the undiluted adjuvant over  
151 time or during a simulated aging process, Examining changes in particle size over time or during  
152 a simulated aging process, Assessing changes in the adsorption capacity for a model protein over  
153 time or during a simulated aging process and analyzing XRD patterns at the beginning and end of  
154 the process.

155 Given that adjuvants are used in vaccine formulations and are categorized as injectable products,  
156 they must be fully sterilized and free of any microorganisms. The most common method for  
157 sterilizing adjuvants is steam autoclaving, in which the sample is subjected to a temperature of

108 121°C for 30 or 60 minutes under 1.2 bar of positive pressure. Consequently, aluminum hydroxide  
109 adjuvants synthesized for vaccine formulations inevitably undergo significant aging during the  
110 sterilization process.

111 Burrell et al. (13) reported that if aluminum hydroxide samples are sterilized at 121°C for 30 or 60  
112 minutes, their structure becomes somewhat more ordered. However, they did not observe a  
113 significant impact of this limited structural change on protein adsorption capacity. Similar  
114 observations were reported by Yu et al. (14) for Alhydrogel® samples. Nevertheless, it is evident  
115 that if milder sterilization conditions are selected, and factors such as zeta potential adjustment,  
116 stirring during the process, and rapid cooling after sterilization are utilized, autoclaving can be  
117 used as a method to prevent crystal growth in aluminum hydroxide.

118 The aim of this study is to investigate the aging process of aluminum hydroxide adjuvant,  
119 focusing on the changes that occur in key parameters such as pH, particle size, protein adsorption  
120 capacity, and XRD patterns. Considering that aging is inherently a long-term process, a thermal  
121 treatment method was utilized to simulate aging within a shorter timeframe. By subjecting the  
122 adjuvant to controlled heating at 100°C for durations of 24, 48, and 72 hours, this study aimed to  
123 replicate the structural and physicochemical changes typically observed during prolonged  
124 storage. This approach provides a practical and accelerated model for understanding the factors  
125 influencing the stability and functionality of aluminum hydroxide adjuvants.

126  
127 In this study, aluminum hydroxide adjuvant was subjected to aging simulation at pH levels of 5,  
128 6, 7, and 8, as well as in a solution containing 8.5 g/L sodium chloride with a pH of 7, for durations  
129 of 24, 48, and 72 hours at 100°C. Additionally, from each series, one sample was sterilized using  
130 steam autoclaving at 121°C for 15 minutes. Immediately after the sterilization cycle, the samples  
131 were rapidly cooled with agitation.

132 Subsequently, changes in pH, particle size, and protein adsorption capacity were measured. XRD  
133 patterns were obtained for the initial samples, 72-hour-aged samples, and sterilized samples from  
134 each series. The results showed that samples maintained at higher pH levels experienced more  
135 pronounced structural changes due to the aging process, which was confirmed by the XRD  
136 patterns. Similarly, an increase in particle size was observed in the samples that were more  
137 significantly affected by aging. A parallel trend was also noted in the reduction of protein  
138 adsorption capacity.

189 Increasing the ionic strength of the adjuvant solution by adding sodium chloride weakens dipole  
190 interactions and reduces the zeta potential of particles in these samples. Consequently, the aging  
191 process was observed to be significantly slower in samples with higher ionic strength.

192  
193 For the sterilized samples, the reduced sterilization time of 15 minutes and the use of agitation  
194 during cooling disrupted crystal growth. This intervention resulted in XRD patterns that were more  
195 similar to those of amorphous structures. However, these changes during the sterilization process  
196 did not have a significant impact on protein adsorption capacity, and the samples remained within  
197 the defined standard limits.

198  
199 **2. Material and methods**

### 200 **2.1. Materials**

201 This study utilized aluminum hydroxide adjuvant produced by the Razi Vaccine and Serum  
202 Research Institute (Karaj, Iran), which was prepared and concentrated as a 1.65% solution. BSA  
203 was purchased from Merck (Darmstadt, Germany).

204 Additionally, the following chemical compounds were used in the synthesis process:

- 205 • Ammonium sulfate, batch number 17465103, purchased from Scharlau, molecular biology  
206 grade.
- 207 • Aluminum ammonium sulfate (dodecahydrate), batch number 20445101, purchased from  
208 Scharlau, extra pure grade.
- 209 • Ammonia solution (25%), batch number 3333, purchased from Merck.

### 210 **2.2 Apparatus**

- 211 • XRD analysis was performed using a D8 Bruker Advance X-ray Diffractometer.
- 212 • Protein adsorption measurements were conducted at a wavelength of 280 nm using a UV-  
213 160A Shimadzu UV-Visible Spectrophotometer.
- 214 • Particle size determination was carried out using a Zetasizer Nano ZS 90.

### 215 **2.3. Preparation of Aluminum Hydroxide Gel**

216 To synthesize the aluminum hydroxide adjuvant, an ammonium sulfate solution was first used to  
217 create a buffered environment, maintaining the pH between 8 and 9 by adding ammonium  
218 hydroxide solution. Subsequently, with vigorous stirring, an aluminum ammonium sulfate solution

was rapidly introduced. The stoichiometric ratios were carefully adjusted to ensure that the final pH of the reaction remained between 7.5 and 8.

After 1 hour of continuous stirring, the mixture was allowed to stand to facilitate the formation of a gel phase while a clear supernatant layer developed. The next step involved decanting the supernatant liquid to remove excess ammonium sulfate. The gel was then washed until the ammonium ion concentration was reduced to 50 ppm and the sulfate ion concentration to 100 ppm. Finally, the gel concentration was adjusted to 1.65% dry matter.

#### **2.4. Sampling and Experimental Design**

Initially, the primary aluminum hydroxide gel was adjusted to pH levels of 5, 6, 7, and 8, and the samples were coded based on their pH (for example series 5 refer samples with initial pH=5). Additionally, a sample with a pH of 7 was prepared by adding 8.5 gr L<sup>-1</sup> of NaCl, and this sample was coded as Z. This sample was specifically prepared to evaluate the effect of increased ionic strength on the aging process.

Considering that the aging process can be simulated by maintaining the samples at 100°C for a specified duration, the samples were stored at this temperature for 24, 48, and 72 hours. Furthermore, one sample from each batch was subjected to steam autoclaving at 121°C for 15 minutes to study the effect of the autoclave process on aging. Immediately after the sterilization cycle, the samples were stirred, and their temperature was rapidly brought down to room temperature.

The collected samples were sequentially analyzed for pH changes, particle size variations, BSA adsorption capacity, and finally, their XRD patterns were extracted.

#### **2.5. Sampling and Experimental Design**

The primary aluminum hydroxide gel was adjusted to pH levels of 5, 6, 7, and 8, and the samples were coded accordingly (e.g., series 5 refers to samples with an initial pH of 5). Additionally, to evaluate the effect of increased ionic strength, a sample with a pH of 7 containing 8.5 g/L of NaCl was prepared and coded as Z.

Since the aging process can be simulated by thermal treatment, the samples were stored at 100°C for 24, 48, and 72 hours. Furthermore, one sample from each batch was subjected to steam autoclaving at 121°C for 15 minutes to evaluate the effect of sterilization on aging. Immediately after the sterilization cycle, the samples were stirred, and their temperature was rapidly brought down to room temperature.

## 2.6. Analytical Methods

The collected samples were sequentially analyzed for:

1. pH changes
2. Particle size variations
3. BSA adsorption capacity
4. XRD patterns

## 2.7. Justification for the 72-Hour Aging Study

Aging is a long-term process that occurs over weeks or months in real storage conditions. However, to accelerate and simulate this process in a shorter timeframe, a thermal treatment approach at 100°C was employed for 24, 48, and 72 hours. This method aligns with previous studies where controlled thermal conditions were used to induce and analyze structural changes in aluminum hydroxide adjuvants.

Additionally, this timeframe was selected based on the fact that significant structural transformations, including changes in pH, particle size, and protein adsorption capacity, were observed within this period. However, it is acknowledged that further studies involving longer storage durations under standard conditions are necessary for a more comprehensive aging profile. It is important to note that the aging process is inherently a time-dependent phenomenon, but the objective of this study was not to determine the stability or shelf life of the adjuvant. Instead, this research aimed to analyze the aging trends and the structural changes occurring during the process. By studying these trends, valuable insights can be gained into the physicochemical changes that take place and their impact on protein-based vaccine formulations. Furthermore, the study provides a basis for proposing strategies to slow down or even halt the aging process, ensuring better formulation stability and efficacy in vaccine development.

## 3. Results and Discussion

### 3.1. pH Changes Analysis

Fig. 1 illustrates the pH changes in different samples after 24, 48, and 72 hours of storage at 100°C. The results indicate that samples with higher initial pH values experience more significant pH changes. These changes can be attributed to the chemical equilibrium of the reaction described in Equation (1). At higher pH levels, the reaction tends to release more  $H^+$ , leading to a greater decrease in pH. Consequently, samples with an initial pH of 8 exhibit the most pronounced pH changes compared to other samples.

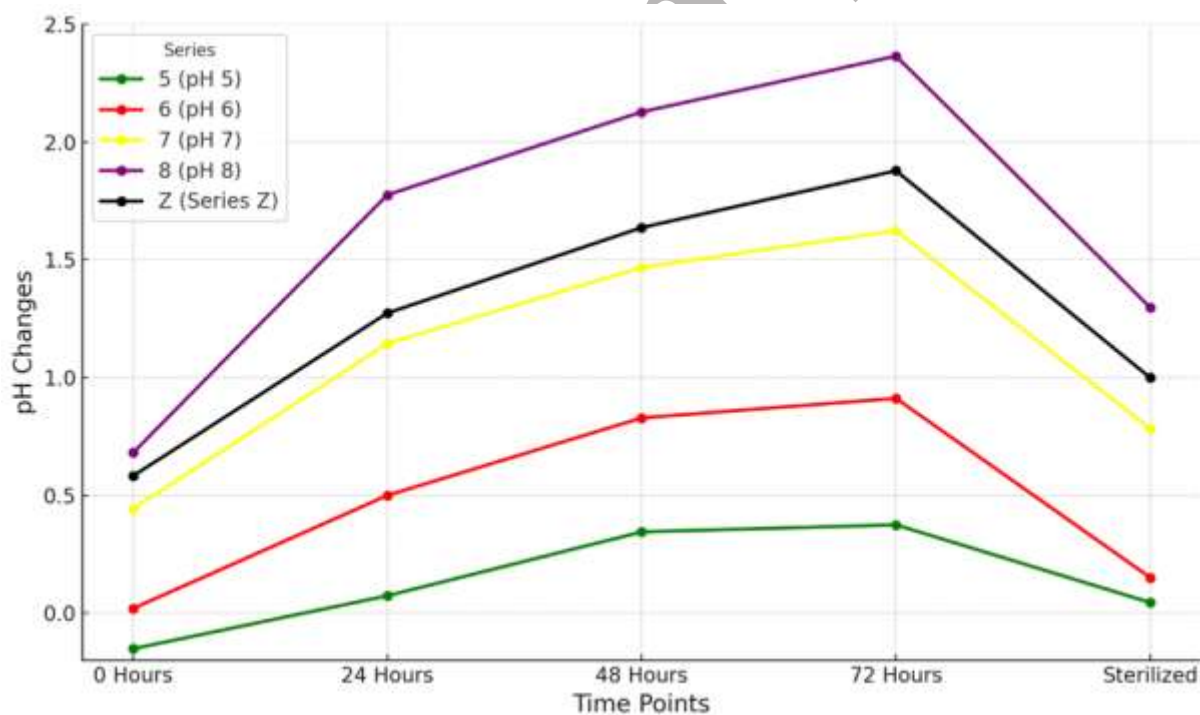
281 Comparing the graphs of the Z and 7 series samples (Fig. 1) reveals that the pH changes in the Z  
282 series samples are slightly more substantial, despite both series having the same initial pH of 7.  
283 This discrepancy is likely due to the higher ionic strength in the Z series, which reduces the activity  
284 of the  $H^+$  ions produced during the reaction described in Equation (1). As a result, the reaction  
285 proceeds further in the Z series, generating more  $H^+$  ions and leading to greater pH changes.

286 An intriguing observation is that in all sample series, the pH changes in the sterilized samples are  
287 negligible compared to their initial values (hour 0). This finding suggests that the autoclaving  
288 process under the described conditions significantly slowed the reaction outlined in Equation (1).

289 This slowdown can be attributed to the following factors:

- 290 1) The reduced sterilization time of 15 minutes, which limited the extent of the reaction.
- 291 2) Continuous agitation during the cooling phase and rapid cooling, which disrupted the  
292 crystallization process and preserved the amorphous structure of the samples.

293



294

295

Fig. 1. pH Changes Over Time

296

297

### 298 3.2. Particle Size Changes

299 Fig. 2 illustrates the changes in particle size across different samples. As outlined in Equation  
300 (1), at higher pH levels, the reaction responsible for forming double hydroxide bridges  
301 progresses more rapidly, releasing more  $H^+$ . The continuation of this reaction facilitates the  
302 formation of additional double hydroxide bridges, which leads to an increase in particle size over  
303 time.

304 When comparing samples Z and 7, Fig. 1 previously showed that the pH change in sample Z was  
305 greater than in sample 7, attributed to the reaction described in Equation (1) producing more  $H^+$   
306 ions in the Z series due to its higher ionic strength. However, Fig. 2 reveals an interesting trend:  
307 the particle size in sample Z is smaller compared to sample 7. This apparent discrepancy can be  
308 explained by considering the role of ionic strength. In sample Z, the increased ionic strength  
309 reduces electrostatic interactions between particles, as described in Equation (2). This reduction  
310 slows the rate of particle aggregation and the formation of double hydroxide bridges, despite the  
311 higher proton production observed in sample Z.

312 These findings highlight the complex interplay between ionic strength, particle aggregation, and  
313 reaction progression in the formation of aluminum hydroxide adjuvants. While the progression  
314 of the reaction in Equation (1) leads to pH changes and potential particle growth, the influence  
315 of ionic strength significantly moderates particle size by mitigating inter-particle attractions. This  
316 underscores the importance of controlling ionic strength in optimizing adjuvant properties for  
317 vaccine formulations.



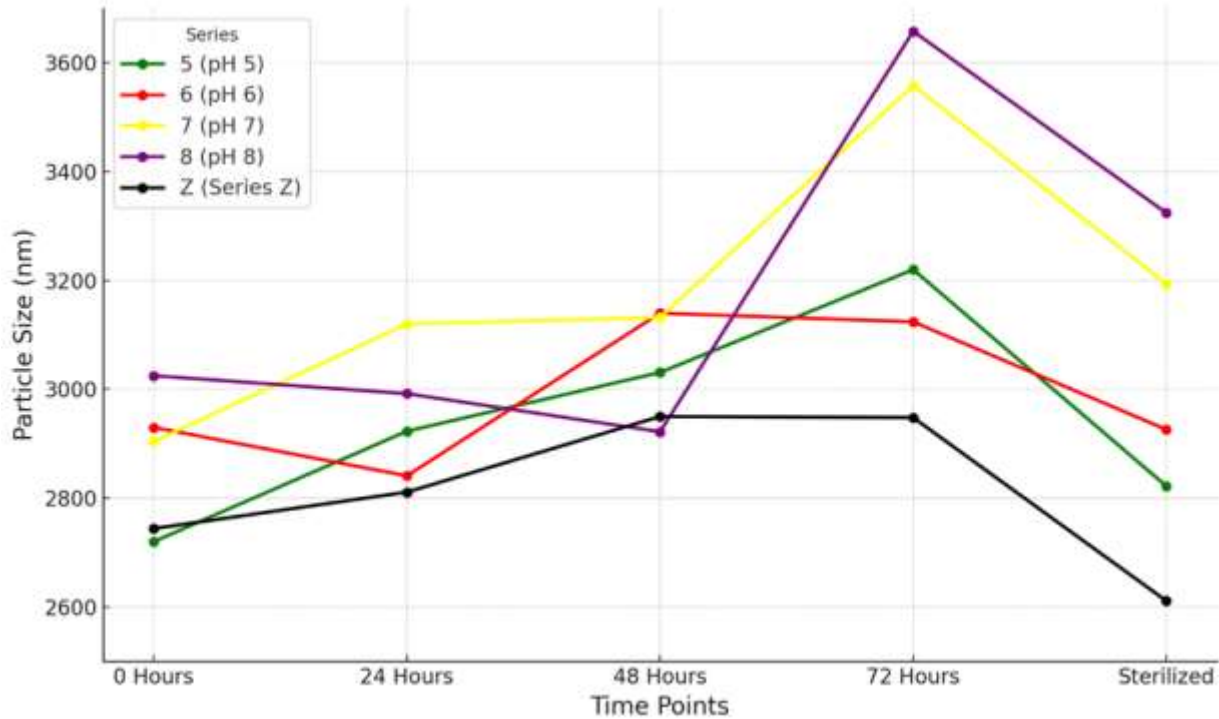


Fig. 2 Particle Size (nm) Over Time

318

319

320

### 3.3. Changes in Protein Adsorption Capacity

321 In this experiment, BSA was used as the model protein due to its isoelectric point of 4.8, in contrast  
 322 to the isoelectric point of aluminum hydroxide, which is 11. Fig. 3 shows the percentage of BSA  
 323 adsorption at a concentration ratio of one milligram of aluminum to four milligrams of BSA.  
 324

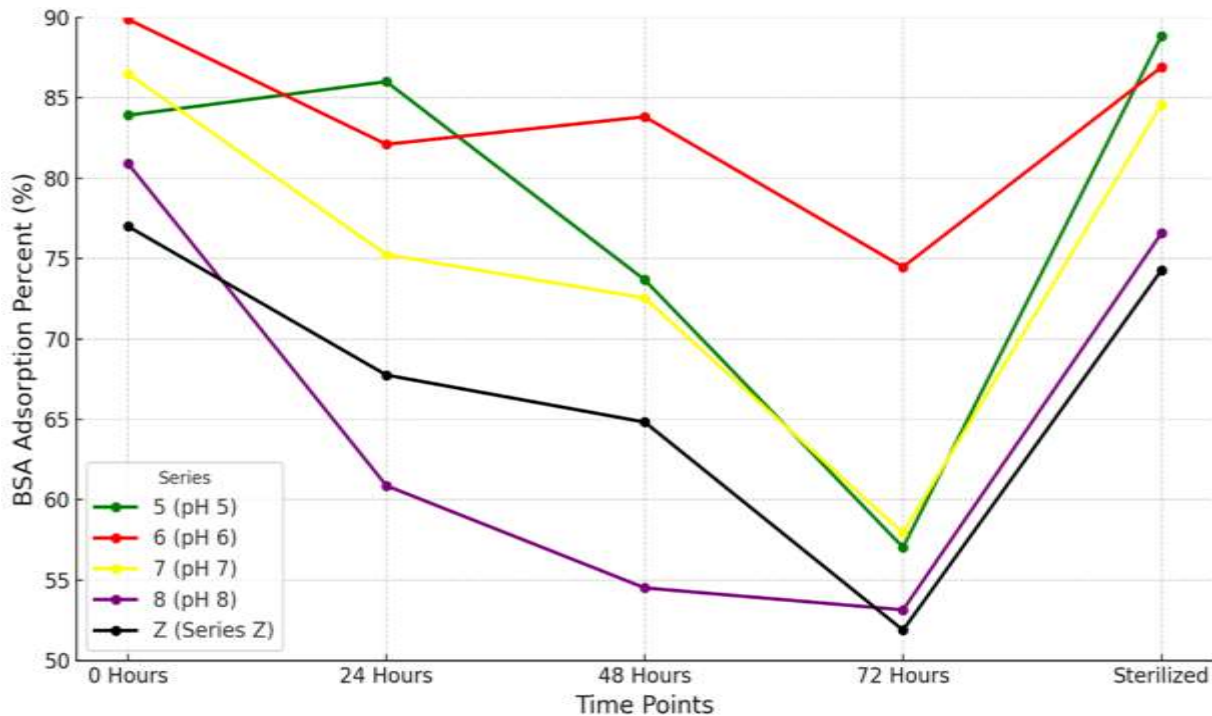
325 As observed in Figures 1 and 2, the effects of the aging process were more pronounced in samples  
 326 with higher pH. Consequently, aged samples showed a greater loss in protein adsorption capacity  
 327 compared to non-aged samples. This trend is generally evident in Fig. 3, where samples with lower  
 328 pH demonstrate a better ability to adsorb proteins.

329 Interestingly, in sample Z, despite the reduction in particle size, there was no corresponding  
 330 increase in protein adsorption capacity. This can be attributed to the fact that particle size is only  
 331 one of the factors influencing protein adsorption. The reduction in electrostatic interactions due to  
 332 a lower zeta potential in sample Z resulted in diminished protein adsorption capacity. In this  
 333 context, the increased ionic strength, while moderating particle aggregation as shown earlier,  
 334 adversely affected protein adsorption by reducing the effective binding forces between the protein

330 molecules and the adjuvant surface. Thus, although sample Z underwent less aging, it exhibited a  
336 greater reduction in protein adsorption capacity.

337 The sterilized samples, as illustrated in Fig. 3, retained a significant portion of their initial protein  
338 adsorption capacity. Measures taken during sterilization, including reducing the sterilization time  
339 and stirring during the cooling phase, were effective in mitigating the aging effects. These  
340 interventions disrupted crystallization processes, preserved the surface reactivity of the adjuvant,  
341 and thereby maintained its protein adsorption capacity.

342 These findings highlight the intricate balance between ionic strength, surface properties, and  
343 protein adsorption in optimizing aluminum hydroxide adjuvants. Maintaining proper ionic  
344 conditions and using precise sterilization protocols can significantly enhance the functionality of  
345 adjuvants in vaccine formulations.



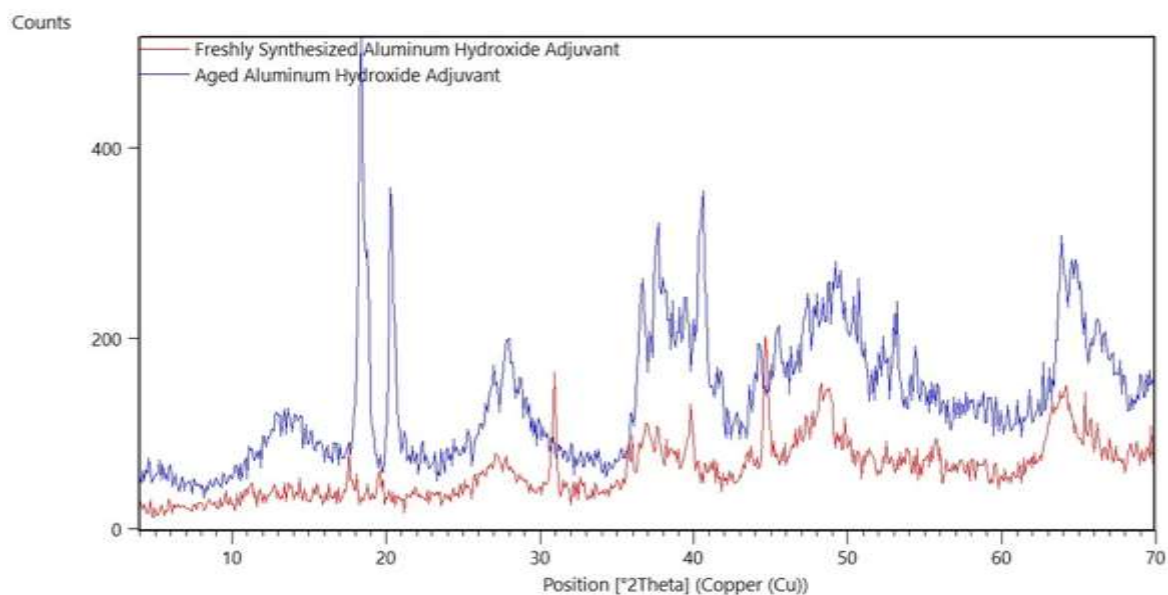
346  
347 Fig. 3. BSA Adsorption Percent at 280 nm in  $1\text{ mg } Al^{+3} / 4\text{ mg } BSA$

### 348 349 3.4. XRD Pattern Analysis

350 In Fig. 4, the XRD pattern of freshly synthesized aluminum hydroxide adjuvant, which has  
351 undergone minimal aging, is shown in blue, while the XRD pattern of the aged sample is  
352 represented in red. The pattern of the aged sample features sharp, high-intensity peaks, indicating

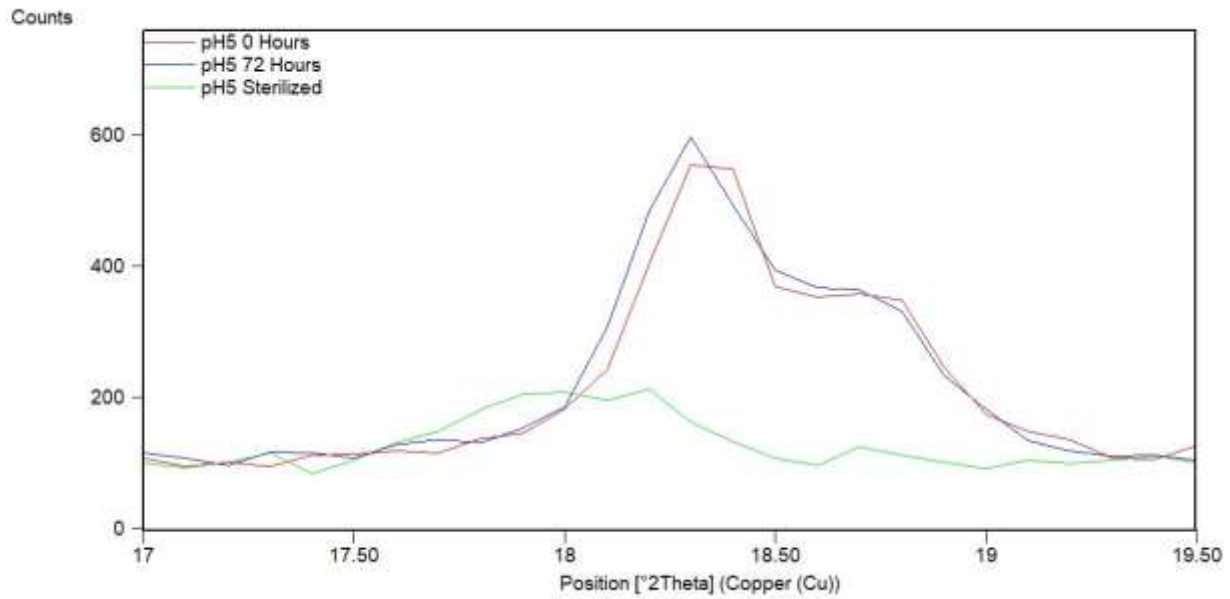
303 an increase in structural order and crystallinity. This pattern closely resembles the XRD profile  
304 of AlOOH.

305 In contrast, the XRD pattern of the freshly prepared adjuvant shows broad, low-intensity peaks,  
306 suggesting that the structure remains disordered. This pattern aligns well with the profile of  
307 amorphous aluminum hydroxide.



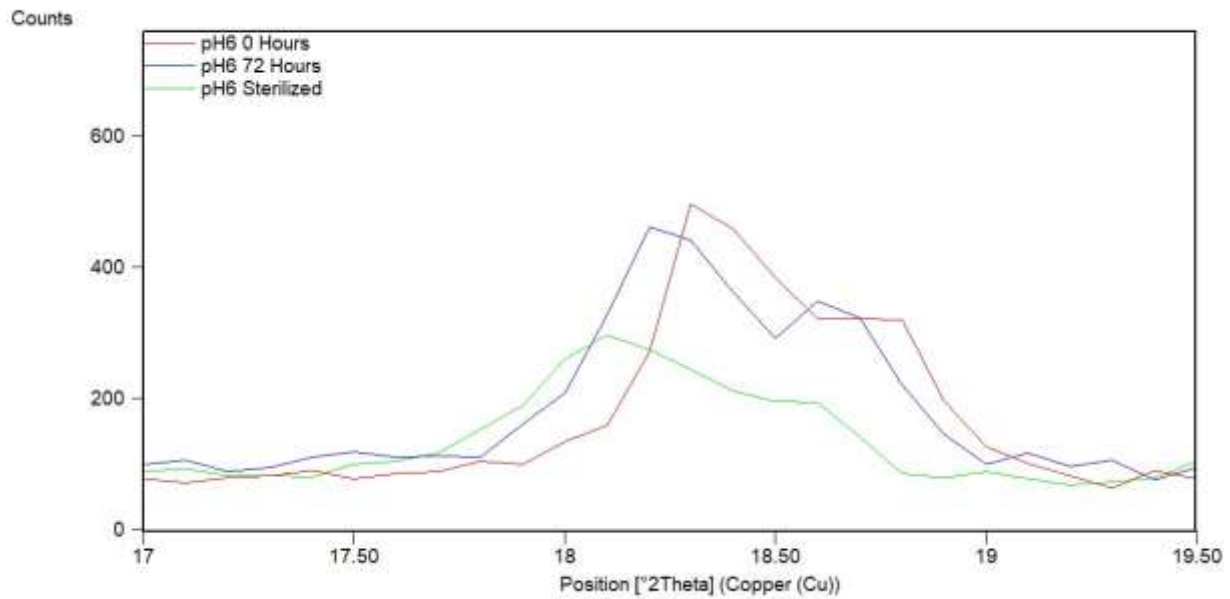
308  
309 Fig. 4. XRD pattern of freshly synthesized aluminum hydroxide adjuvant and aged aluminum hydroxide  
310 adjuvant

361 In Fig. 5, the XRD patterns of the samples in the range of 17 to 19.5 degrees 2θ are compared,  
362 highlighting the changes in samples subjected to a 72-hour thermal treatment, sterilized samples,  
363 and initial samples at the same pH.



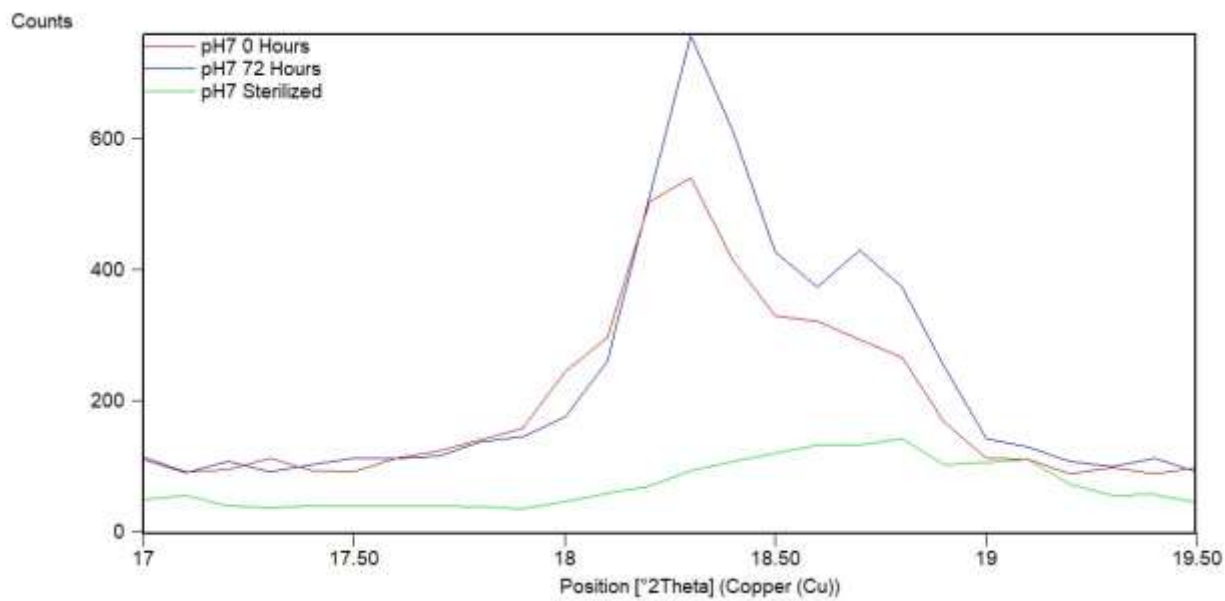
364  
365

Fig. 5a. XRD patterns of pH 5 series in the range of 17 to 19.5 degrees 2θ



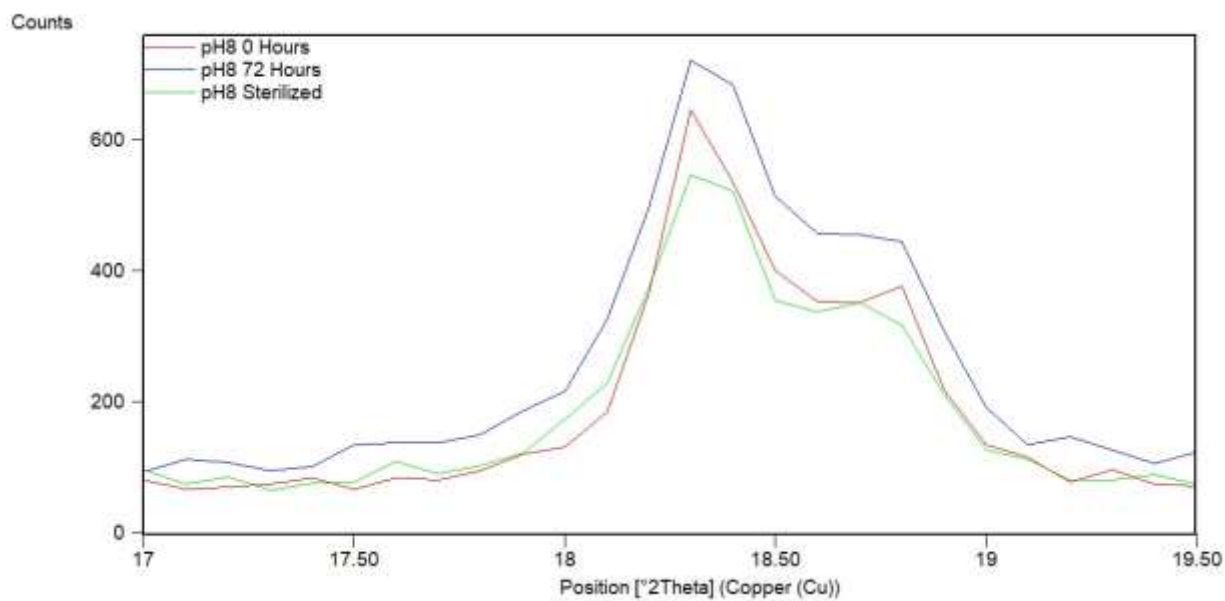
366  
367

Fig. 5b. XRD patterns of pH 6 series in the range of 17 to 19.5 degrees 2θ



۳۶۸  
۳۶۹

Fig. 5c. XRD patterns of pH 7 series in the range of 17 to 19.5 degrees 2θ



۳۷۰  
۳۷۱

Fig. 5d. XRD patterns of pH 8 series in the range of 17 to 19.5 degrees 2θ

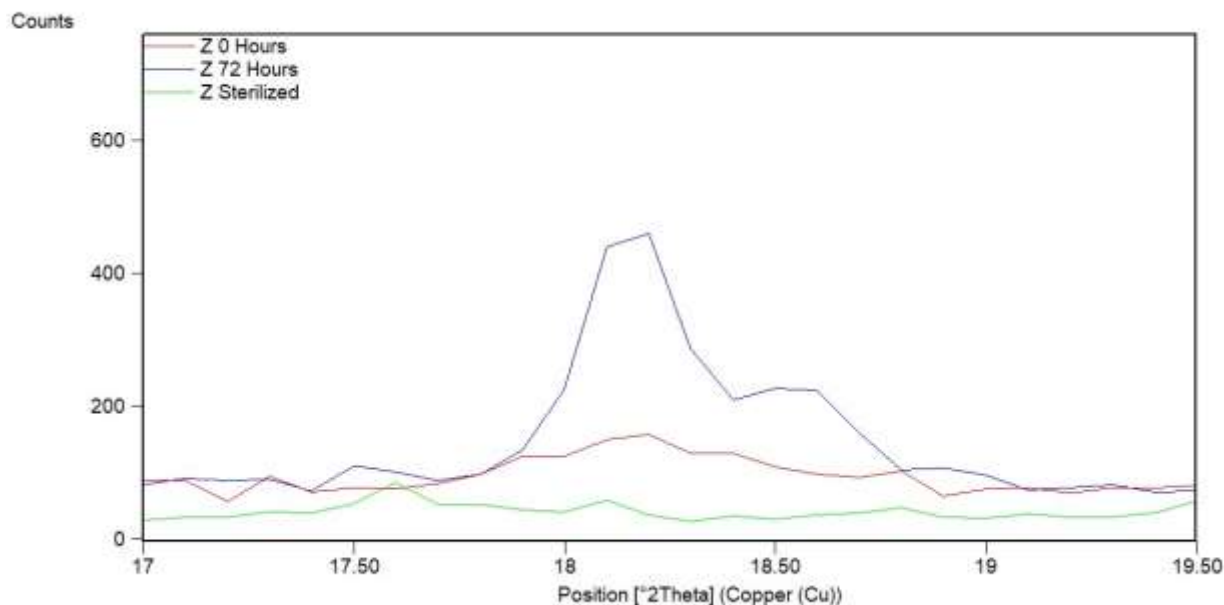


Fig. 5e. XRD patterns of Z series in the range of 17 to 19.5 degrees  $2\theta$

372  
373  
374  
375  
376  
377  
378  
379  
380  
381  
382  
383  
384  
385  
386  
387  
388  
389  
390

It is observed that in all samples, sterilization under the described conditions leads to the transformation of the semi-crystalline structure towards an amorphous state. As a result, the peaks in the sterilized patterns are broader and less intense. In the pH 7 sample and the sterilized **Z** sample, the structure is notably more similar to an amorphous form.

Furthermore, it is observed that thermal treatment across all series results in increased structural order, transforming the samples into a semi-crystalline AlOOH form. Samples with higher pH exhibit greater crystallinity.

#### 4. Discussion

The aging process induces significant structural changes in aluminum hydroxide adjuvants, primarily through the formation of double hydroxide bridges, leading to a decrease in pH and an increase in particle size. These structural changes are clearly observable through XRD patterns. Additionally, the increased structural order and formation of semi-crystalline structures due to aging contribute to reduced protein adsorption capacity, ultimately diminishing the adjuvanticity of the adjuvant.

391 Sterilization, a critical step in vaccine production, poses challenges as it can accelerate aging  
392 effects and increase structural ordering, as reported by Barrell et al. (13) and Yu et al. (14).  
393 However, the innovative strategies employed in this study—such as reducing sterilization time to  
394 15 minutes, continuous agitation during the cooling phase, and rapid cooling post-sterilization—  
395 successfully mitigated these aging effects. These measures disrupted crystallization, preserved the  
396 amorphous structure of the adjuvant, and produced finer particles, aligning with methodologies  
397 used in nano-adjuvant synthesis.

398  
399 The findings also revealed that maintaining the adjuvant at a pH of 5 and increasing the ionic  
400 strength of the solution effectively reduced crystallization tendencies and preserved adjuvanticity.  
401 The minimal pH changes observed in sterilized samples provide compelling evidence of the  
402 importance of optimized sterilization protocols. These results highlight that maintaining pH  
403 stability is crucial for ensuring the structural integrity of protein-based antigens, minimizing  
404 aggregation, and achieving consistent adjuvant performance. Furthermore, the findings align with  
405 previous studies, including those by Yu et al. (14), demonstrating that autoclaving under controlled  
406 conditions stabilizes the structure of aluminum hydroxide adjuvants and prevents crystallization.  
407 This underscores the critical role of balancing ionic strength and refining sterilization techniques  
408 to enhance vaccine stability and performance.

409  
410 Overall, despite the observed aging effects, aluminum hydroxide adjuvant samples produced under  
411 the experimental conditions maintained their quality within defined standards. However, these  
412 findings underscore the need for further optimization of storage conditions and handling practices  
413 to minimize aging-related reductions in protein adsorption capacity and adjuvanticity.

## 414 **5. Conclusion**

415 This study demonstrated that the aging process significantly affects the structural and  
416 physicochemical properties of aluminum hydroxide adjuvants, including reductions in pH,  
417 increases in particle size, and declines in protein adsorption capacity. These changes can adversely  
418 impact the adjuvanticity of aluminum hydroxide. Nevertheless, strategies such as reducing  
419 sterilization time, increasing ionic strength, and maintaining optimal pH effectively mitigated these  
420 effects, preserving the stability and functionality of the adjuvant.

421 The observed stability of sterilized samples, particularly their minimal pH changes, is a significant  
422 finding for vaccine formulations. Maintaining pH stability ensures the integrity of protein antigens,  
423 reduces aggregation, and enhances adjuvant performance, ultimately contributing to vaccine  
424 efficacy. The alignment of these results with prior research on ionic strength and sterilization (13),  
425 (14) provides strong evidence for the practical application of these approaches in vaccine  
426 development.

427 Although this study was limited to a 72-hour simulation of aging, it provided valuable insights into  
428 short-term structural changes and their implications. Future research should explore the long-term  
429 effects of aging under real-world storage conditions to develop a more comprehensive aging  
430 profile.

431 This research enhances our understanding of aluminum hydroxide adjuvants and provides practical  
432 solutions for optimizing their performance in protein-based vaccine formulations. These findings  
433 can guide the development of more stable and effective vaccine formulations, reinforcing the role  
434 of aluminum hydroxide as a gold-standard adjuvant in vaccine production.

#### 435 **Author contributions**

436 Study concept and design: M. Z.

437 Acquisition of data: M. Z. And M.N. and M.R.H. and S.Z. and S.B.

438 Analysis and interpretation of data: M. Z. and M.R.H and S.Z.

439 Drafting of the manuscript: M. Z.

440 Critical revision of the manuscript for important intellectual content: M. Z. and M.R.H. and S.Z.

441 Administrative, technical, and material support: M.R.H.

442 Study supervision: M. Z. and M.R.H.

443

#### 444 **Acknowledgements**

445 Financial support for this project was provided by the Research Council of Razi Vaccine and  
446 Serum Research Institute (RVSRI)

447

#### 448 **References**

449 1. World Health Organization (WHO). Message by the Director of the Department of  
450 Immunization, Vaccines and Biologicals at WHO [Internet]. 2024. Available from:  
451 [https://www.who.int/news/item/31-01-2024-message-by-the-director-of-the-department-of-](https://www.who.int/news/item/31-01-2024-message-by-the-director-of-the-department-of-immunization)  
452 immunization

2. World Health Organization (WHO). Counting the impact of vaccines: For a safer, healthier world [Internet]. 2021. Available from: <https://www.who.int/news/item/22-04-2021-counting-the-impact-of-vaccines>
3. Centers for Disease Control and Prevention (CDC). Vaccine-Preventable Diseases. Global Immunization Strategic Framework [Internet]. 2024. Available from: <https://www.cdc.gov/globalhealth/immunization>
4. Wang Z, Li S, Shan P, Wei D, Hao S, Zhang Z, Xu J. Improved aluminum adjuvants eliciting stronger immune response when mixed with hepatitis B virus surface antigens. *ACS Omega*. 2022;7:34528-34537.
5. Glenny AT, Pope CG, Waddington H, Wallace U. Immunological notes. XVII–XXIV. *J Pathol Bacteriol*. 1926;29:31–40.
6. Ghimire TR. The mechanisms of action of vaccines containing aluminum adjuvants: an in vitro vs in vivo paradigm. *SpringerPlus*. 2015;4:181. doi:10.1186/s40064-015-0972-0.
7. Laera D, HogenEsch H, O’Hagan DT. Aluminum Adjuvants—‘Back to the Future.’ *Vaccines*. 2022;10(7):1099. doi:10.3390/vaccines10071099.
8. Burrell LS, White JL, Hema SL. Stability of aluminium-containing adjuvants during aging at room temperature. *Vaccine*. 2000;18(21):2188-2192.
9. Yau KP, Schulze DG, Johnston CT, Hem SL. Aluminum hydroxide adjuvant produced under constant reactant concentration. *J Pharm Sci*. 2006;95(12):2731-2738. doi:10.1002/jps.20692.
10. Johnston CT, Wang SL, Hem SL. Measuring the surface area of aluminum hydroxide adjuvant. *J Pharm Sci*. 2002;91(7):1703-1711. doi:10.1002/jps.10141.
11. Dandashli EA, Zhao Q, Yitta S, Morefield GL, White JL, Hem SL. Effect of thermal treatment during the preparation of aluminum hydroxide adjuvant on the protein adsorption capacity during aging. *Pharm Dev Technol*. 2002;7(4):401-406.
12. Rinella JV Jr, White JL, Hem SL. Effect of anions on model aluminum adjuvant-containing vaccines. *J Colloid Interface Sci*. 1998;205:161–165.
13. Burrell LS, Lindblad EB, White JL, Hem SL. Stability of aluminium-containing adjuvants to autoclaving. *Vaccine*. 1999 Jun 4;17(20-21):2599-603. doi: 10.1016/s0264-410x(99)00051-1.
14. Yu G, Yang W, Zhang N, Yang C, Zeng H, Xue C, Sun B. Autoclave-Induced Changes in the Physicochemical Properties and Antigen Adsorption of Aluminum Adjuvants. *Pharmaceutical Nanotechnology*. 2023. doi:<https://doi.org/10.1016/j.xphs.2023.10.009>.

ελε

ελσ **Figure Legends**

ελς **Fig 1** pH Changes Over Time

ελϕ **Fig 2** Particle Size Over Time

ελϘ **Fig 3** BSA Adsorption Percent at 280 nm in  $1 \text{ mg Al}^{+3} / 4 \text{ mg BSA}$

ελϙ **Fig 4** XRD pattern of freshly synthesized aluminum hydroxide adjuvant and aged aluminum hydroxide adjuvant

ελϛ **Fig 5 a** XRD patterns of pH 5 series in the range of 17 to 19.5 degrees 2θ

ελϜ **Fig 5 b** XRD patterns of pH 6 series in the range of 17 to 19.5 degrees 2θ

ελϝ **Fig 5 c** XRD patterns of pH 7 series in the range of 17 to 19.5 degrees 2θ

ελϞ **Fig 5 d** XRD patterns of pH 8 series in the range of 17 to 19.5 degrees 2θ

ελϠ **Fig 5 e** XRD patterns of Z series in the range of 17 to 19.5 degrees 2θ

ελϡ

٤٩٧ Table 1. Data of pH Changes Over Time

Series	0 Hours	24 Hours	48 Hours	72 Hours	Sterilized
5 (pH 5)	-0.151	0.074	0.345	0.375	0.045
6 (pH 6)	0.02	0.5	0.829	0.912	0.151
7 (pH 7)	0.443	1.145	1.468	1.624	0.783
8 (pH 8)	0.681	1.776	2.128	2.365	1.297
Z (Series Z)	0.583	1.274	1.637	1.878	0.999

٤٩٨

٤٩٩ Table 2. Data of Particle Size (nm) Over Time

Series	0 Hours	24 Hours	48 Hours	72 Hours	Sterilized
5 (pH 5)	2720	2923	3031	3220	2822
6 (pH 6)	2930	2841	3140	3124	2926
7 (pH 7)	2904	3120	3132	3558	3194
8 (pH 8)	3025	2992	2922	3658	3324
Z (Series Z)	2744	2811	2950	2948	2611

٥٠٠

٥٠١

٥٠٢ Table 3. BSA Adsorption Percent at 280 nm in  $1 \text{ mg Al}^{+3} / 4 \text{ mg BSA}$

Series	0 Hours	24 Hours	48 Hours	72 Hours	Sterilized
5 (pH 5)	83.92%	86.01%	73.68%	57.04%	88.86%
6 (pH 6)	89.89%	82.11%	83.83%	74.48%	86.91%
7 (pH 7)	86.50%	75.25%	72.55%	57.93%	84.59%
8 (pH 8)	80.92%	60.88%	54.52%	53.15%	76.58%
Z (Series Z)	77.01%	67.76%	64.83%	51.89%	74.28%

٥٠٣